

# Experimental Teleportation of a Quantum Controlled-NOT Gate

Yun-Feng Huang<sup>1</sup>, Xi-Feng Ren<sup>1</sup>, Yong-Sheng Zhang<sup>1</sup>, Lu-Ming Duan<sup>2,1</sup>, and Guang-Can Guo<sup>1</sup>

<sup>1</sup>*Laboratory of Quantum Information, University of Science and Technology of China, Hefei, Anhui 230026, P. R. China*

<sup>2</sup>*Department of Physics and FOCUS center, University of Michigan, Ann Arbor, MI 48109*

Teleportation of quantum gates is a critical step for implementation of quantum networking and teleportation-based models of quantum computation. We report an experimental demonstration of teleportation of the prototypical quantum controlled-NOT (CNOT) gate. Assisted with linear optical manipulations, photon entanglement produced from parametric down conversion, and coincidence measurements, we teleport the quantum CNOT gate from acting on local qubits to acting on remote qubits. The quality of the quantum gate teleportation is characterized through the method of quantum process tomography, with an average fidelity of 0.84 demonstrated for the teleported gate.

**PACS numbers:** 03.67.Lx, 03.67.Hk, 03.65.Od, 42.50.-P

Physical implementation of quantum computation requires coherent manipulation of a large number of quantum bits. To scale up the number of qubits in real physical systems, a particularly interesting approach is to connect individual physical setups together through some quantum communication channels and perform distributed quantum computation over all the nodes [1,2]. Such a quantum networking approach has provided practical scaling methods for several promising candidate systems for implementation of quantum computation [3,4]. For instance, in trapped ion or cavity quantum-electrodynamical (QED) systems, the number of qubits inside an individual trap or cavity could be limited from some practical considerations, but the limitation can be overcome by wiring up those individual systems through photon connection [3,4].

Distributed quantum computation requires one to perform collective quantum gates on remote qubits. The best way to achieve that is through quantum teleportation [5], i.e., one can teleport a collective quantum gate from acting on local qubits to acting on remote qubits [6,7,4]. Teleportation of quantum states has been demonstrated in several physical systems [11], from a photon to a photon, or from an atom to an atom. However, teleportation of collective quantum gates is more challenging than teleportation of quantum states. For instance, if one wants to achieve a remote quantum controlled-NOT (CNOT) gate by teleporting the quantum state back and forth, one needs two rounds of state teleportations and a local CNOT gate, which consumes two ebits (entanglement bits), four cbits (classical bits), and several local collective operations. A better way to achieve nonlocal quantum CNOT gate on remote qubits is through direct teleportation of quantum gates [6,4]. The minimum communication cost for teleportation of a quantum CNOT

gate is one ebit and two cbits [7].

Here, we report an experiment which demonstrates complete teleportation of the prototypical quantum CNOT gate on photonic qubits. Through linear optical manipulation and with assistance of entanglement generated from spontaneous parametric down conversion (SPDC), we teleport a local CNOT gate, which acts on polarization and path qubits of a single photon, to a remote CNOT gate, acting on polarization qubits of two distant photons. The quality of the quantum gate teleportation is characterized through quantum process tomography [8], which allows one to fully construct the teleported quantum gate operation by measurement of its effects on a series of basis states. Through this method, we demonstrate that the teleported quantum CNOT gate has a mean fidelity of 0.84, averaged over all the input states. With linear optical manipulations, quantum CNOT gates on different photons have also been directly demonstrated in the coincidence basis by several recent experiments [9,10]. The demonstration of teleportation of the quantum CNOT gate, apart from its fundamental interest, is a significant step towards realization of quantum networking [3,4] and teleportation-based models of quantum computation [12–14].

First, we briefly explain the basic idea of teleportation of quantum gate operations [6,7,4]. Assume that we have two parties, Alice and Bob, each having two qubits 1,2 and 3,4 (see Fig. 1). We have a shared EPR state  $|\Phi\rangle_{23} = \frac{1}{\sqrt{2}}(|00\rangle_{23} + |11\rangle_{23})$  between the qubits 2 and 3, and our purpose is to perform a nonlocal quantum CNOT gate on the qubits 1 and 4 with assistance of this shared EPR state, local gate operations on qubits 1,2 and 3,4, and classical communications. The input state of the qubits 1,4 is arbitrary, expressed in general as  $|\Psi\rangle_{14} = d_0|00\rangle_{14} + d_1|01\rangle_{14} + d_2|10\rangle_{14} + d_3|11\rangle_{14}$ . To achieve the goal, we first perform a quantum CNOT gate  $C_{12}$  (where the first subscript of  $C$  denotes the control qubit and the second is the target qubit) on the local qubits 1,2, and then teleport this gate from the qubits 1,2 to the qubits 1,4 through the gate teleportation. The gate teleportation is possible because of the following identity [4]

$$\begin{aligned} C_{34}C_{12}(|\Psi\rangle_{14} \otimes |\Phi\rangle_{23}) &= |0+\rangle_{23} \otimes C_{14}(|\Psi\rangle_{14}) \\ &\quad + |0-\rangle_{23} \otimes \sigma_1^z C_{14}(|\Psi\rangle_{14}) \\ &\quad + |1+\rangle_{23} \otimes \sigma_4^x C_{14}(|\Psi\rangle_{14}) \quad (1) \\ &\quad + |1-\rangle_{23} \otimes (-\sigma_1^z \sigma_4^x) C_{14}(|\Psi\rangle_{14}). \end{aligned}$$

where  $|\pm\rangle_3 = (|0\rangle_3 \pm |1\rangle_3)/\sqrt{2}$ , and  $\sigma_1^z$  and  $\sigma_4^x$  are the

Pauli operators acting on the corresponding qubits. This identity shows that teleportation of the CNOT gate  $C_{12}$  is achieved as follows (illustrated in Fig. 1): first we apply a CNOT gate on the local qubits 3,4, and then measure the qubits 2,3 respectively in the basis  $\{|0\rangle_2, |1\rangle_2\}$  and  $\{|+\rangle_3, |-\rangle_3\}$ . Conditional on the measurement outcomes, we perform one of the following single-bit corrections  $\{I, \sigma_1^z, \sigma_4^x, -\sigma_1^z \sigma_4^x\}$  on the qubits 1,4. The whole procedure teleports the quantum CNOT gate from the local qubits 1,2 to the remote qubits 1,4 ( $C_{12} \rightarrow C_{14}$ ). The teleportation consumes one ebit represented by the state  $|\Phi\rangle_{23}$ , and one cbit in each direction to communicate the measurement outcomes. This procedure has the minimum communication cost for a remote quantum CNOT gate [7].

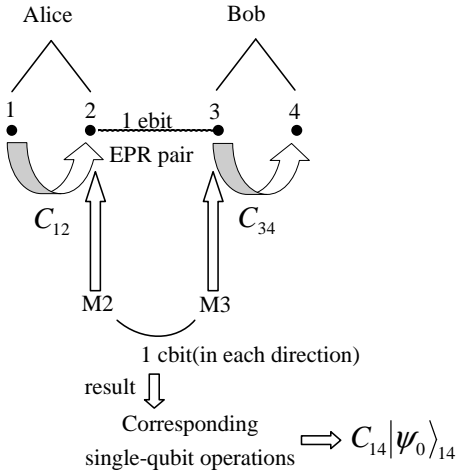


FIG. 1. A sketch to show the idea of teleportation of the quantum CNOT gate. Each dot stands for one qubit. M2 and M3 represent single qubit measurements of qubit 2 and 3 in an appropriate basis, and the measurement outcomes are communicated between Alice and Bob.

To experimentally demonstrate teleportation of the quantum CNOT gate, we need to have the resource for standard teleportation as well as the ability of performing CNOT gates on local qubits. Similar to the state teleportation experiment by the De Martini's group [11], we choose the local qubits represented by the polarization and the path degrees of freedom of a single photon. This allows us to easily perform deterministic CNOT gates on the local qubits through linear optical manipulation. That ability, together with photon entanglement produced from the SPDC setup, allows us to teleport the deterministic CNOT from two local qubits carried by a single photon to nonlocal qubits represented by two remote photons.

Our experimental setup is shown schematically in Fig. 2. A 0.59 mm thick BBO ( $\beta-B_aB_2O_4$ ) crystal arranged in a Kwiat-type configuration [15] is pumped by a 351.1 nm laser beam (100 mW) produced by an  $Ar^+$  laser (Coherent, Sabre, model DBW25/7). Through the SPDC process, photon pairs are generated in an polarization-

entangled EPR state  $(|HH\rangle + |VV\rangle)/\sqrt{2}$ , where  $H$  and  $V$  stand for two orthogonal linear polarizations. To introduce the path qubit, we split each out beam of BBO with a polarizing beam splitter (PBS1 and PBS2), which transmits the horizontally polarized photon ( $|H\rangle$ ) and reflects the vertically polarized photon ( $|V\rangle$ ). The two paths after the PBS are denoted by  $|0\rangle$  and  $|1\rangle$ , respectively. We use a half wave plate (HWP1 and HWP2 in Fig. 2) in the path  $|1\rangle$  to exchange the polarization states  $|V\rangle$  and  $|H\rangle$ . After that, the polarization entanglement is transferred to the path entanglement, with the whole state having the form

$$|\Psi\rangle_{1234} = |H\rangle_1 \left[ (|00\rangle_{23} + |11\rangle_{23})/\sqrt{2} \right] |H\rangle_4, \quad (2)$$

where the subscript denotes different qubits. The qubits 1,2 and 3,4 are carried respectively by the first and the second photons.

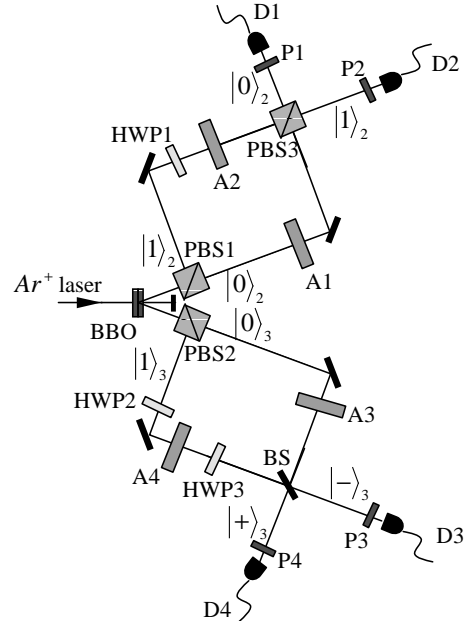


FIG. 2. Schematic experimental setup for teleportation of the quantum CNOT gate. Qubits 1,2 and 3,4 are carried respectively by the polarization and the path degrees of freedom of the upper (1,2) and the lower (3,4) photons. Each of the elements A1-A4 consists of a HWP and a QUWP, used for preparation of arbitrary polarization states. Each of the polarization analyzers P1-P4 also consists of a HWP and a QUWP, which, combined with single photon detectors, measures the photon polarization state in an arbitrary basis.

To demonstrate teleportation of the CNOT gate, we need to measure its effects for an arbitrary input state of the qubits 1 and 4. The qubits 1 and 4 can be prepared in arbitrary polarizations by rotating from the state  $|H\rangle$  with a HWP and a quarter wave plate (QUWP), which are denoted in Fig. 2 as A1, A2, A3, A4 in each path of the photons. The local CNOT gate  $C_{12}$  is achieved by interfering the  $|0\rangle_2$  and  $|1\rangle_2$  paths at a PBS (PBS3), which change the path of photon if it is in the V polar-

ization [16]. To have phase stability, the M-Z interferometer formed by PBS1 and PBS3 is equal-armed. The other local CNOT  $C_{34}$  is simply realized by putting a HWP (HWP3, set at  $45^\circ$ ) in the  $|1\rangle_3$  path, to reverse the polarization state of qubit 4 if qubit 3 is in the state  $|1\rangle$ .

The next step is to perform measurement of qubit 2 and 3 respectively in the basis  $\{|0\rangle, |1\rangle\}$  and  $\{|+\rangle, |-\rangle\}$ . The measurement of qubit 2 is easily done by detecting two outputs of PBS3 with a single-photon detector. The measurement of qubit 3 requires another interference of the photon paths  $|0\rangle_3$  and  $|1\rangle_3$  at a 50/50 beam splitter (BS) before the single-photon detection. The M-Z interferometer formed by PBS2 and BS is also equal-armed. We then register the four possible coincidences D1-D4, D1-D3, D2-D4, D2-D3 from the four single-photon detectors (D1 to D4), corresponding detection of the states  $|0\rangle_2|+\rangle_3$ ,  $|0\rangle_2|-\rangle_3$ ,  $|1\rangle_2|+\rangle_3$ , and  $|1\rangle_2|-\rangle_3$ , respectively. Before each single-photon detector, we insert a polarization analyzer (P1 to P4). By recording the change of coincidence counts with rotation of P1-P4, we construct the final polarization state of qubits 1 and 4 through quantum state tomography [17].

TABLE 1:

P1,P2 settings	Coinc. Counts(10s)	P1,P2 settings	Coinc. Counts(10s)
HH	765	DH	1221
HV	891	DV	277
HD	731	DD	745
HR	13	DR	712
VH	848	RH	741
VV	850	RV	923
VD	876	RD	1448
VR	1763	RR	767

FIG. 3. The coincidence counts of the detectors D1 and D4 for a period of 10 seconds with 16 different settings of the polarization analyzers P1 and P4. The input state of qubits 1 and 4 is given by  $|R\rangle_1|R\rangle_4$ . The corresponding density matrix constructed from these data is shown in Fig. 4a.

To confirm that the local gate  $C_{12}$  has been teleported to a remote gate  $C_{14}$ , we verify that the teleported gate generates entanglement between qubits 1 and 4 from a product input state  $|\Psi_{in}\rangle_{14} = |R\rangle_1|R\rangle_4$ , where  $|R(L)\rangle = (|H\rangle + (-i)V\rangle)/\sqrt{2}$ . If teleportation is perfect, we should get an entangled output state  $|\Psi_{out}\rangle_{14} = C_{14}|\Psi_{in}\rangle_{14} = (|H\rangle_1|R\rangle_4 - |V\rangle_1|L\rangle_4)/\sqrt{2}$ . We construct the real density matrix  $\rho_{14}^{\text{real}}$  of qubits 1 and 4 by measuring the coincidences D1-D4 with 16 different settings of the polarization analyzers P1 and P4, with the results shown in Table 1. From the data, with the standard method of quantum state tomography [17], we construct the measured density matrix  $\rho_{14}^{\text{real}}$ , with its real and imaginary elements shown in Fig. 4. The results are compared with those from the ideal density matrix  $\rho_{14}^{\text{ideal}} = |\Psi_{out}\rangle_{14}\langle\Psi_{out}|$ . We find from the data that the state fidelity  $F_s \equiv_{14} \langle\Psi_{out}|\rho_{14}^{\text{real}}|\Psi_{out}\rangle_{14} \simeq 0.81$ , which

significantly exceeds the criterion of  $F_s = 0.5$  for demonstration of entanglement of the state  $\rho_{14}^{\text{real}}$  [20]. With similar methods, we have also measured the output state fidelity when qubits 1,4 are input with one of the basis states  $|HH\rangle, |HV\rangle, |VH\rangle, |VV\rangle$ , with the results given respectively by  $F_s^{HH} = 0.97, F_s^{HV} = 0.97, F_s^{VH} = 0.99, F_s^{VV} = 0.98$ .

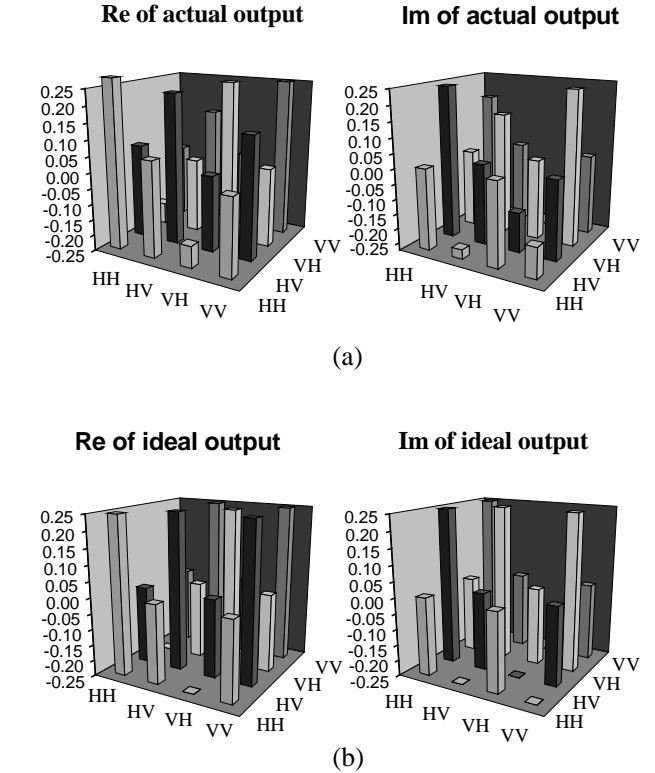


FIG. 4. (a). The real and the imaginary parts of the output density matrix reconstructed from the coincidence data in Table 1. (b). The corresponding density matrix elements in the ideal case with a CNOT gate acting on the input state  $|R\rangle_1|R\rangle_4$ .

To fully characterize the teleported quantum gate, one would like to construct from measurements the corresponding super-operator through the method of quantum process tomography (QPT) [18,19]. The QPT of the quantum CNOT gate requires us to measure the output density matrices corresponding to 16 different input states of qubit 1 and 4 [19], respectively given by  $|HH\rangle, |HV\rangle, |HD\rangle, |HR\rangle, |VH\rangle, |VV\rangle, |VD\rangle, |VR\rangle, |DH\rangle, |DV\rangle, |DD\rangle, |DR\rangle, |RH\rangle, |RV\rangle, |RD\rangle, |RR\rangle$ , where  $|D\rangle = (|H\rangle + |V\rangle)/\sqrt{2}$ . The reconstruction of each output density matrix requires 16 coincidence measurements. So, in total we get  $16 \times 16$  coincidence data. The quality of a quantum gate is measured by the so-called process fidelity  $F_P$  (or called gate fidelity), which is defined as the overlap of the matrices corresponding respectively to the measured and the ideal super-operators [19]. From the  $16 \times 16$  coincidence data [21], we find  $F_P \simeq 0.80$  for our experiment. An interesting result deduced from

the process fidelity  $F_P$  is the average gate fidelity  $\bar{F}$ , which is defined as the state fidelity between the measured and the ideal outputs of the CNOT gate, averaged over all possible input states. There is a simple relation between  $\bar{F}$  and  $F_P$ , given by  $\bar{F} = (dF_P + 1)/(d + 1)$ , where the dimension  $d = 4$  for the CNOT gate [19]. So, we conclude that  $\bar{F} \simeq 0.84$  for our experiment.

The measured fidelity in our experiment is pretty high. The remaining imperfection comes from two main sources. The first contribution is from imperfection of the two M-Z interferometers, whose visibility is about 85%. The second source is that the EPR state generated from SPDC is not perfect. We measured the visibility of the polarization entanglement in the two-photon state right after SPDC, which is as high as 98.2%; but through the state tomography analyses, we find there are still non-negligible unwanted elements arising from the measured density matrix compared with the ideal EPR state, which affect our experiment result.

In summary, we have demonstrated teleportation of the quantum CNOT gate by using photon entanglement generated from SPDC and linear optical manipulations. We use dual qubit representation for each single-photon, which allows us to perform local deterministic CNOT gate. This local gate is then teleported to a remote gate acting on two distant photons. The quality of the gate teleportation is characterized through the comprehensive quantum state and process tomography techniques, and an average teleported gate fidelity as high as 0.84 is confirmed from the measured data.

This work was supported by the Chinese National Fundamental Research Program (2001CB309300), the National Natural Science Foundation (No. Grant 60121503), the NSF of China (10304017), the Innovation funds from Chinese Academy of Sciences. LMD acknowledges supports from the ARDA under ARO contract, the FOCUS seed funding, and the A. P. Sloan Fellowship.

- (1997); J. F. Poyatos, J. I. Cirac, and P. Zoller, Phys. Rev. Lett. **78**, 390 (1997).
- [9] T. B. Pittman, B. C. Jacobs, and J. D. Franson, Phys. Rev. Lett. **88**, 257902 (2002); K. Sanaka, K. Kawahara, and T. Kuga, Phys. Rev. A **66**, 040301(R) (2002); T. B. Pittman *et al.*, Phys. Rev. A **68**, 032316 (2003); J. L. O'Brien *et al.*, Nature, **426**, 264 (2003).
  - [10] S. Gasparoni *et al.*, Phys. Rev. Lett. **93**, 020504 (2004); Z. Zhao *et al.*, e-print *quant-ph/0404129*.
  - [11] D. Bouwmeester *et al.*, Nature **390**, 575 (1997); D. Bochi *et al.*, Phys. Rev. Lett. **80**, 1121 (1998); A. Furusawa *et al.*, Science **282**, 706 (1998). M. A. Nielsen *et al.*, Nature **396**, 52 (1998); Y.-H. Kim *et al.*, Phys. Rev. Lett. **86**, 1370 (2001); M. Riebe *et al.*, Nature **429**, 734 (2004); M. D. Barrett *et al.*, Nature **429**, 737 (2004).
  - [12] D. Gottesman and I. L. Chuang, Nature **402**, 390 (1999).
  - [13] R. Raussendorf and H. J. Briegel, Phys. Rev. Lett. **86**, 5188 (2001).
  - [14] E. Knill, R. Laflamme, and G. J. Milburn, Nature **409**, 46 (2001).
  - [15] P. G. Kwiat *et al.*, Phys. Rev. A **60**, R773 (1999).
  - [16] N. J. Cerf, C. Adami, and P. G. Kwiat, Phys. Rev. A **57**, R1477 (1998).
  - [17] A. G. White, D. F. V. James, P. H. Eberhard, P. G. Kwiat, Phys. Rev. Lett. **83**, 3103 (1999).
  - [18] A. G. White *et al.*, e-print *quant-ph/0308115*.
  - [19] J. L. O'Brien *et al.*, e-print *quant-ph/0402166*.
  - [20] B. B. Blinov *et al.*, Nature **428**, 153 (2004).
  - [21] The  $16 \times 16$  coincidence data is too lengthy to be listed here. It is available on the website <http://202.38.83.245/james/data.ps>.

- 
- [1] J. I. Cirac, A. K. Ekert, S. F. Huelga, and C. Macchiavello, Phys. Rev. A **59**, 4249 (1999).
  - [2] D. P. DiVincenzo, Fortschr. Phys. **48**, 771-783 (2000).
  - [3] J. I. Cirac, P. Zoller, H. J. Kimble, and H. Mabuchi, Phys. Rev. Lett. **78**, 3221-3224 (1997).
  - [4] L.-M. Duan *et al.*, *quant-ph/0401020*, Quant. Inf. Comput. **4**, 165 (2004).
  - [5] C. H. Bennett *et al.*, Phys. Rev. Lett., **70**, 1895 (1993).
  - [6] M. A. Nielsen, I. L. Chuang, Phys. Rev. Lett. **79**, 321 (1997); A. S. Sørensen, K. Mølmer, Phys. Rev. A **58**, 2745 (1998); D. Gottesman, *quant-ph/9807006*.
  - [7] D. Collins, N. Linden, and S. Popescu, Phys. Rev. A **64**, 032302 (2001); J. Eisert *et al.*, Phys. Rev. A **62**, 052317 (2000).
  - [8] I. L. Chuang and M. A. Nielsen, J. Mod. Opt. **44**, 2455